Continuous Fluidized Bed Drying With and Without Internals: Kinetic Model

C. Srinivasakannan,[a,*] **Ahmed Al Shoaibi,**[a] **and N. Balasubramanian**[b]
[a]Chemical Engineering Department, The Petroleum Institute, Abu Dhabi, UAE
[b]Chemical Engineering Department, Anna University, Chennai, India

Spirals as internals are utilized to reduce the axial mixing of solids in fluidized beds, by routing the solids flow in a predetermined route or by localizing the solids mixing. The drying kinetics of continuous fluidized bed with and without internals has been compared and modeled using batch drying kinetics and residence time distribution analysis. The batch drying experiments were conducted to establish the drying kinetics of ragi mimicking the conditions in the continuous fluidized bed. The batch drying kinetic data was modeled using a number of semi empirical models to identify the appropriate model and establish the kinetic parameters. Among the models tested, the Page model was found to match the experimental data, with minimum error. The kinetic parameter (k) was found to increase with temperature. The activation energy (E) was estimated to be 30.5kJ mol^{-1}, while the Arrhenius constant was 0.03 s^{-1}. The drying rate in the continuous bed was found to increase with increase in temperature of the heating medium and height of the downcomer. The rate of drying in a continuous fluidized bed is lower than the rate of drying in batch fluidized bed, while the drying rate in a continuous fluidized bed with internals approximates drying rate in batch fluidized bed.

Key words:
Fluidized bed, drying kinetics, spiral internals, food grain drying

Introduction

Fluidized beds are one of the preferred modes of contact between gas-solid, gas-liquid and gas-liquid-solid operations in industries with the application ranging from simple adsorbers, wastewater systems to complex reactors. Fluidized beds find increasing application in the drying of agricultural material although they are being widely used in industries for drying of fertilizers, chemicals, pharmaceuticals and minerals. The increasing application of fluidized bed drying for agricultural materials is due to the evolving designs of fluidized bed for fluidization of coarse material, which is rather difficult to fluidize. Fluidized beds, as compared to other modes of drying, offer advantages such as high heat capacity of the bed, improved rates of heat and mass transfer between the phases, and ease in handling and transport of fluidized solids.[1]

The mixing pattern in continuous fluidized beds is expected to resemble a continuous stirred tank reactor (CSTR), with the rate of drying in continuous fluidized bed lower than that of batch fluidized bed. Hence, attempts were made to reduce the axial mixing of the solid phase with internals by localizing the solids mixing. Internals in addition to reducing the axial dispersion, contribute to the reduction in bubble size by breaking them or preventing coalescence, thereby enhancing the transfer between the phases.

Some of the commonly used internals are spirals, multistage etc.[2–4] The present investigation utilizes a spiral internal in which the solids flow along the length of the spiral, from the entry to the exit. The choice of using a spiral internal was based on the ease with which to fabricate and attach the spiral to the air distributor plate. The solids moisture content in a fluidized bed without internal is uniform at any point within the bed, while it varies continuously along the flow path in the spiral fluidized bed reflecting plug flow conditions. The solid mixing is localized to reduce the axial mixing of solids in the bed. The pressure drop in a spiral internal bed is of same magnitude as that of continuous single-stage fluidized beds, while that of the multistage internals increases with the number of stages. The back mixing in gas phase is negligible, and it can be considered to exhibit a near perfect plug flow.

Knowledge of drying kinetics is essential for the design of dryers. The complex hydrodynamics and process calculations are material and dryer specific, rendering development of numerous mathematical models for drying kinetics. These range from analytical models solved with a variety of simplified assumptions to purely empirical models, often built by regression of experimental data. A detailed analysis of the various modeling efforts on drying kinetics in batch fluidized beds has been reported in literature.[5] The knowledge on drying kinetics in continuous fluidized beds is limited to the

*Corresponding author: csrinivasakannan@pi.ac.ae

popularly known continuous single-stage fluidized bed and its performance is often modeled using the residence time distribution of solids in the bed.[3]

The variation in bed temperature of batch drying with respect to the continuous drying has been reported to be a source of error in utilizing batch kinetics to model the continuous drying.[6] In order to reduce the variations between batch and the continuous drying, the solids holdup and the bed height were kept identical in both cases in the present study. As the prediction of drying kinetics in continuous bed largely depends on the accuracy in modeling of the batch kinetic data, a precise model is very important. In general, the modeling of drying kinetics is believed to adhere to constant rate period followed by a falling rate period distinguished by hypothetical critical moisture content. The prediction of critical moisture content, the equilibrium moisture content along with utilization of two different models for the different sections of the drying kinetic curve all cumulate to larger prediction errors. The present study ignores the conventional approach to modeling the batch kinetics as reported earlier[7] due to the accuracy of prediction.

The objectives of the present study were to experimentally investigate the drying kinetics of ragi (Eleusine Corocana) in continuous fluidized bed with and without internals, and assess the effect of operating parameters such as temperature, flow rate of the drying medium and bed height of solids. The drying kinetics in continuous fluidized bed is modeled using the residence time distribution of solids and drying kinetics in batch fluidized bed under identical conditions of operation. It is further attempted to test the drying kinetic data with the models reported in the literature.[5,8,9]

Materials

Ragi (Eleusine Corocana) is one of the principal cereal crops in India, Sri Lanka, and East Africa. In India, it is cultivated on more than 2.5 million hectares of land annually. Although it does not enter international markets, it is a very important cereal grain in areas of adaptation. The grain is higher in protein, fat and minerals than rice, corn, or sorghum.[10] The ear heads are gathered when they ripen, and the practice among farmers is to stack the just cut ragi until the cold weather gives way to sunshine. By the time ragi is threshed, it starts developing molds. Fresh ragi without molds, as received from the farm, is utilized for drying in the present study. Table 1 lists the physical properties of the ragi, as well as the experimental conditions observed in the present study. A properly dried ragi

T a b l e 1 – *Characteristics of the material and range of experimental parameters covered in the present study*

Name of material	Ragi (Eleusine Corocana)
Shape of material	Spherical
Size, $d_p \cdot 10^3$, m	1.48
Particle density, kg m^{-3}	1200
Minimum fluidization velocity, u_{mf}, m s^{-1}	0.47
Terminal velocity, u_t, m s^{-1}	6.9
Temperature of fluidizing air, °C	60, 70, 80
Fluidizing air velocity, m s^{-1}	1.2
Solid holdup, kg	1.3, 2.6

grain can be stored even up to 50 years necessitating the importance of drying.[11]

Experimental methods

Drying experiments were conducted using fluidized columns of 0.245 m in internal diameter with a height of 0.6 m. Fig. 1(a) shows the schematic of the experimental setup used for batch and continuous drying experiments. A larger column was chosen in order to accommodate the internals in the distributor plate, to favor ease of fabrication and handling. The gas distributor (6) was 2 mm thick with 2 mm perforations having 13 % free area. A fine wire mesh was spot welded over the distributor plate to arrest the flow of solids from the fluidized bed into the air chamber. Air from the blower with volumetric discharge capacity of 200 m^3 h^{-1}, was metered using a calibrated orifice meter (2) before being heated and fed to the fluidization column (7) through the air chamber (5). The electrical heater (3) consists of three heating elements with 2 KW rating. The temperature controller (3) facilitated the control of air temperature within ±2 °C of the set temperature. Air at desired temperature and flow rate was allowed to flow through the fluidization column. The column additionally had a hopper with vibratory feeder (9) and a solids feed tube (10). The downcomer pipe (11) facilitated the variation of the height of solids and solids holdup in the bed, which was located diametrically opposite the solid feed tube (10). The orifice in the exit of the feed hopper and the frequency of vibration were altered to vary the solids rate of flow into the fluidization column. The solids flow rate was varied between 1.8 to 13 g s^{-1} in order to capture the variation of drying rate with the mean residence
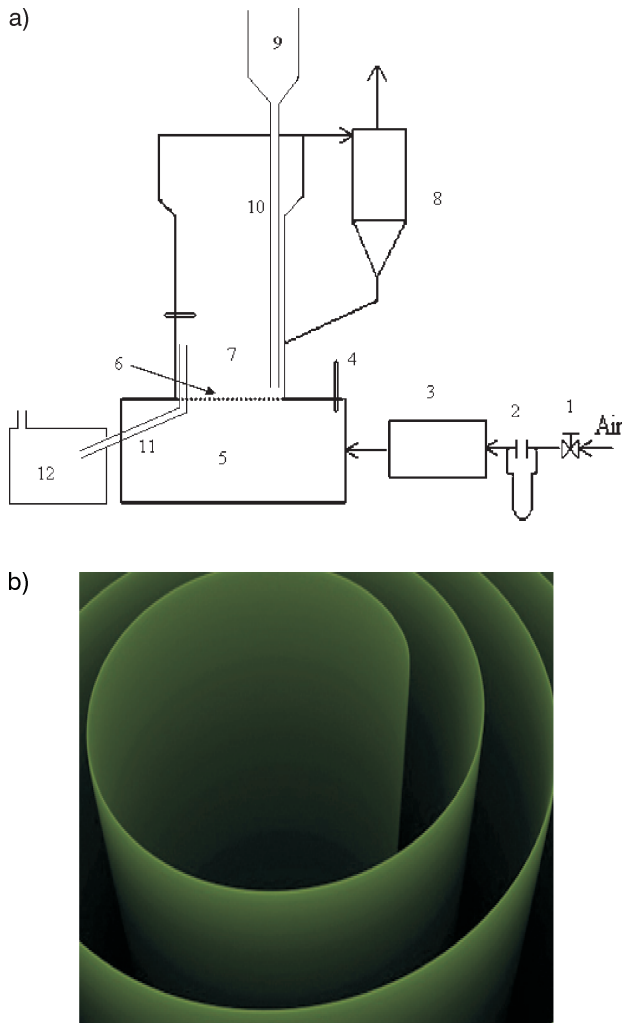
a)

b)

F i g . 1 − *(a) Schematic of the experimental set up: 1. Air control valve, 2. Manometer, 3. Air heater and controller, 4. Thermocouple, 5. Flow normalizing chamber, 6. Air distributor, 7. Fluidization zone, 8. Cyclone, 9. Solids hopper with vibratory feeder, 10. Solids entry downcomer, 11. Solids exit downcomer, 12. Product receiving chamber; (b) Schematic of the spiral internals*

time of solids. The solids holdup and in turn the solids residence time in the bed was altered significantly by varying the downcomer pipe height. The dried samples were withdrawn under steady state condition from the solids outflow pipe, to estimate the moisture content.

In the case of batch experiments, the solids feed tube (10), the downcomer pipes (11), facilitating material inflow and outflow, were removed. A known quantity of ragi with known initial moisture content was introduced into the column after ensuring steady temperature and air flow-rate. Samples were scooped out of the bed at regular time intervals for estimation of moisture. The solids holdup and other experimental conditions were chosen to match the drying conditions in the continuous bed.

For continuous fluidized beds with internals, 1mm thick copper foil (Fig. 1(b) was rolled in the form of a spiral within the circular cross section of the fluidization column and attached to the air distributor plate. The width between the two leaves of the spiral was maintained at 25 mm. The solids were allowed to enter at the center of the column and exit after traversing the entire length of the spiral through the downcomer pipes (Fig. 1(c)). The samples were withdrawn at steady-state condition and the solids holdup was measured by simultaneously stopping the inlet and outlet solids flow from the fluidized bed. The entire amount of solids from the bed was discharged and weighed to estimate the solids holdup.

A good fluidization behavior with reference to perfect mixing of the bed material was observed visually. Ragi can be classified as Geldart B type material that possesses good fluidization characteristics based on its density and size (Table 2). This was substantiated with low fluctuation in the bed pressure drop, which was an indication of smooth fluidization without formation of slugs. The moisture content of ragi was determined based on the difference in initial mass of the sample to the completely dried sample (by drying the samples until constant mass in an air oven at 105 °C). The moisture contents were expressed on dry basis as kilograms of moisture per kilogram of dry solid. The experimental data was checked for reproducibility and found to deviate within ±2 %. The equilibrium moisture content was estimated by keeping the samples in a humidity-controlled air chamber at the desired temperatures until no further mass change. The samples were kept as a thin layer and left in the humidity chamber for more than 12 hours to ensure that equilibrium conditions had been attained, uniformly.

T a b l e 2 − *List of various simple models tested with the drying data of the present study*

Name of Model	Model Equation
Lewis Model (**LM**)	$MR = \exp(-kt)$
Page Model (**PM**)	$MR = \exp(-kt^n)$
Henderson and Pabis (**HPB**)	$MR = a \exp(-kt)$
Two-term Exponential Model (**TEM**)	$MR = a \exp(-kt) + (1-a)\exp(-kat)$

Results and discussion

Experimental data were depicted as plots of dimensionless moisture content MR vs. time for batch drying while they were represented as dimensionless moisture content MR vs. mean residence time for continuous drying of solids. The bed

temperature was found to vary from near wet bulb temperature to the inlet temperature of the air in the batch fluidized bed, while the bed temperature was constant in the continuous fluidized bed without internals, and varied along the flow path length of continuous fluidized bed with spiral as internals.

Batch drying

The influence of operating parameters on batch drying kinetics has been well established and it is generally accepted that the drying rate increases with the increase in the inlet air temperature and flow rate, and decreases with the increase in the solids holdup.[12–16] The drying rate was reported to vary with time, with the highest drying rate while the moisture content of the material was high.

It can be noticed from Fig. 2 that the drying rate increased with increase in the temperature of drying medium and drying time. This observation is in qualitative agreement with the literature. In order to estimate the drying kinetics in the batch fluidized bed, the intention was to utilize the batch kinetics to predict the drying kinetics in the continuous fluidized bed. The experimental drying data are converted to dimensionless moisture ratio (MR), defined as,

$$MR = \frac{C - C_e}{C_i - C_e} \qquad (1)$$

for comparison with the various models. The popular empirical models such as Lewis model, Page model, Henderson and Pabis model, Two-term exponential model have been utilized to model the experimental data.[17–22] Although the above-stated models date from long back, they are still being utilized popularly to model drying kinetics, and hence some recent references are presented. The experimental drying rates are fitted with various model equations, by minimizing the Root Mean Square Error (RMSE) between the experimental drying rate and the model equation. The RMSE is defined as,

$$RMSE = \left[\frac{1}{N} \sum_{i=1}^{n} (MR_{\text{pre},i} - MR_{\text{exp},i})^2 \right]^{0.5} \cdot 100 \quad (2)$$
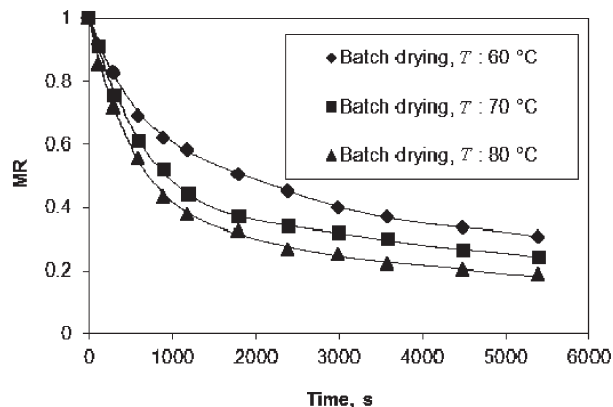

F i g . 2 – *Effect of air temperature on the relative moisture content of solids under batch drying conditions* $C_i = 0.272$; $V_f = 0.06 \ m^3 \ s^{-1}$; $\varepsilon_s = 2.6 \ kg$

where MR refers to moisture ratio, N is the number of data points. The RMSE values for all the semi empirical models were found to be less than 2.7 % with marginal variation in errors between the models. Among the models utilized, the Page model and the Two-term exponential model was found to have less error than the Lewis model and the Henderson Pabis models. The estimated model parameters along with the error limits are listed in Table 3. It has been widely published that among the semi empirical models, the Page model, although simple, is reported to correspond to the experimental data better than other models. It can be seen from Table 3 that the Page model matches the experimental data closely, with lower values of RMSE. Fig. 3 shows the proximity of the Page model with the experimental data. The Page model is a modified version of first-order kinetics (Lewis model) with an index 'n' to the drying time. As compared to all other models, only the Page model has a correction factor to the time variable which could possibly be the reason for its suitability in representing drying kinetics. Earlier investigators have reported the ability of the Page model to closely fit the experimental drying kinetics for mustard, red bell pepper, green pepper.[5,23–25]

The rate constant 'k' used in all the models shows an increase with increase in the inlet temperature of the heating medium. In order to estimate the activation energy and the Arrhenius constant,
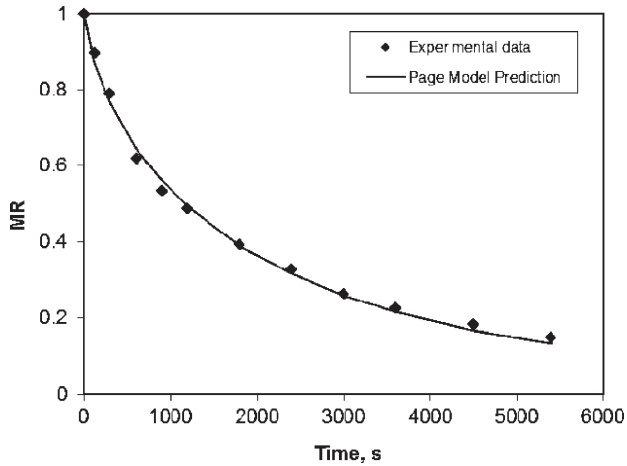
T a b l e   3 – *Evaluated model parameters*

T, °C	PM			LM		TEM			HPB		
	$k \cdot 10^3$	n	RMSE	$k \cdot 10^4$	RMSE	$a \cdot 10$	$k \cdot 10^3$	RMSE	a	$k \cdot 10^4$	RMSE
60	4.9	0.7	1.57	5.15	7.4	1.92	2.09	4.2	0.859	4.0	6.4
70	8.12	0.67	3.1	7.8	8.2	2.41	2.38	5.6	0.850	5.9	8.0
80	8.1	0.695	0.07	9.6	7.6	2.47	2.85	5.3	0.833	7.1	7.7

F i g . 3 – *Comparison of experimental moisture content with the prediction using the Page model*

the Lewis method was chosen, as it represents the well-known first-order kinetics. The Lewis model matches the experimental data within the range of RMSE of 7.4 to 8.2 % in comparison with the Page model, which has RMSE in the range from 1.5 to 3.1 %. Although the RMSE is higher compared to the Page model, the popular first-order kinetics (LM) was chosen to estimate the activation energy.

The activation energy and the Arrhenius constant was estimated using eq. (3), given below,

$$k = k_0 \exp\left[-\frac{E}{R(T + 273.15)} \right] \qquad (3)$$

where E is the activation energy in kJ mol^{-1}, while k_0 is the Arrhenius constant. Fig. 4 shows the plot for estimation of activation energy. The activation energy was found to be 30.5 kJ mol^{-1} and the Arrhenius constant 0.03 s^{-1}. Compared activation energies reported in literature for drying of various bio-products in a hot air thin layer drying were, (i) red pepper from 18.22 to 26.82 kJ mol^{-1},[24] (ii) green bean 35.43 kJ mol^{-1},[26] (iii) corn 29.53 kJ mol^{-1},[27] (iv) soya bean 28.83 kJ mol^{-1},[28] (v) carrot 28.36 kJ mol^{-1}.[29]
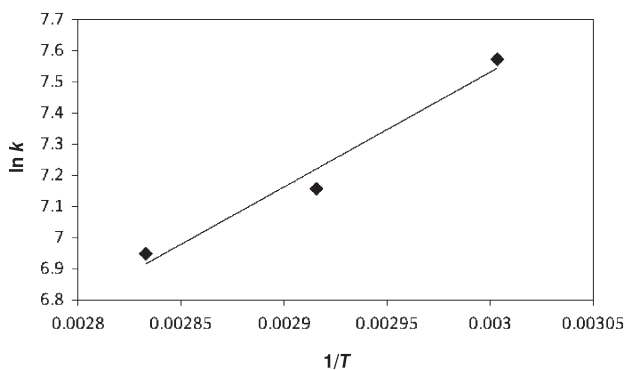

F i g . 4 – *Plot for estimation of activation energy and Arrhenius constant*

Continuous drying of solids

Experiments are conducted to assess the drying kinetics in a continuous fluidized bed with and without internals. The effect of operating variables such as temperature of the inlet air and flow rate of the solids is qualitatively similar in both modes of continuous fluidized bed drying. Fig. 5 shows the effect of inlet air temperature and solids flow rate in a continuous fluidized bed without internals, while Fig. 6 shows the effect of inlet air temperature and solids flow rate in a fluidized bed with spiral internals. An increase in mean residence time could be achieved either by reducing the solids flow rate or by increasing the solids holdup. The mean residence time is defined as the ratio of solids holdup to solids flow rate as detailed below,

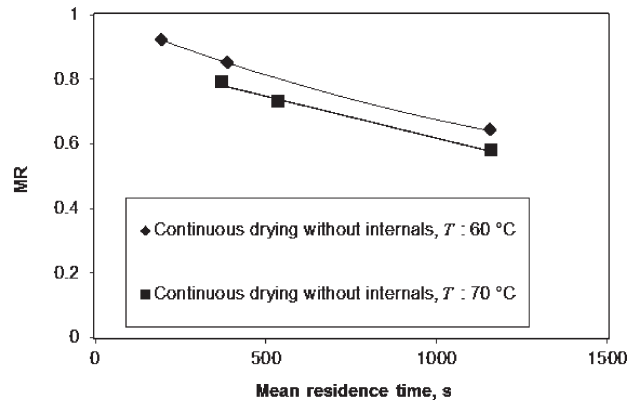$$\bar{t} = \frac{\varepsilon_s}{G_s} \qquad (4)$$

F i g . 5 – *Effect of mean residence time and inlet temperature of air on the relative moisture content of solids leaving the continuous fluidized bed without internals $C_i = 0.3$; $V_f = 0.058$ m^3 s^{-1}; h = 0.068 m*

An increase in temperature of the heating medium would increase the temperature of the material in the bed, which would facilitate faster diffusion of moisture from particle interior to its surface, contributing to the higher drying rate. A comparison between Fig. 5 and Fig. 6 shows that the drying rate is higher in continuous fluidized bed with internals, which could be attributed to the reduction in the axial mixing of solids and reduction in the bubble size in the bed.

Fig.7 shows that the drying rate reduces significantly with increase in the solids holdup. The solids holdup in the bed is influenced by change in flow rates of the phases as well as the height of downcomers. The change in flow rate of the solids is found to marginally increase the solids holdup in the bed, indicating no significant change to the drying rate. However, any alterations to the height of the bed would significantly change the solids
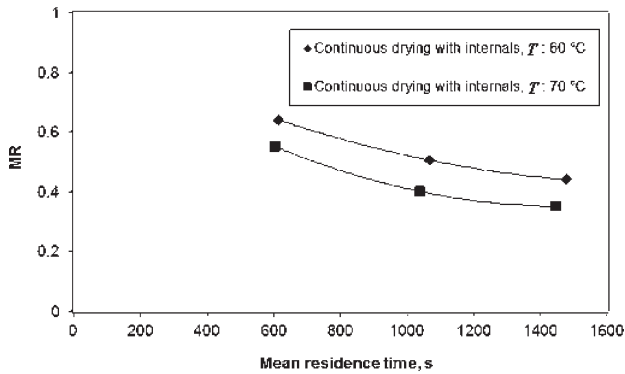
Fig. 6 – *Effect of mean residence time and inlet temperature of air on the relative moisture content of solids leaving the continuous fluidized bed with spiral internal C_i = 0.3; V_f = 0.074 m^3 s^{-1}; h = 0.082 m*
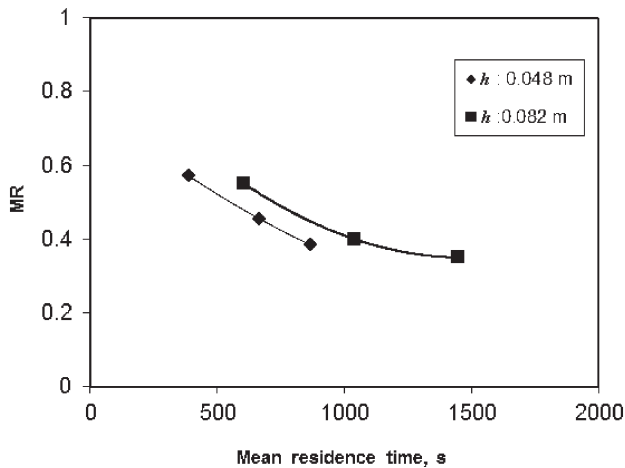

Fig. 7 – *Effect of downcomer height and the mean residence time of solids on the relative moisture content of solids leaving the continuous fluidized bed with spiral internal T_i = 80 °C; V_f = 0.074 m^3 s^{-1}*

Fig. 8 – *Comparison of the relative moisture content of solids in a batch fluidized bed with continuous fluidized bed with and without internals T_i = 70 °C; V_f = 0.06 m^3 s^{-1}*

holdup in the bed. The higher solids holdup on one hand would increase the interfacial area between the heating medium and solids, and reduce on the other hand the proportion of air to solids. The lower air to solids ratio would lead to lower bed temperature, and hence higher moisture content of solids leaving the fluidized bed. This is synonymous with the drying kinetics observed with batch fluidized bed wherein a reduction in the bed temperature with increased solids holdup had been observed. However, it should be remembered that a higher solids holdup results in higher solids residence time, which ultimately results in lower moisture content of the solids leaving the fluidized bed.

Modeling of continuous drying of solids

While comparing the drying kinetics of batch bed with the continuous bed, identical conditions of residence time of solids and solids holdup in the bed is maintained, in both modes. Fig. 8 compre-
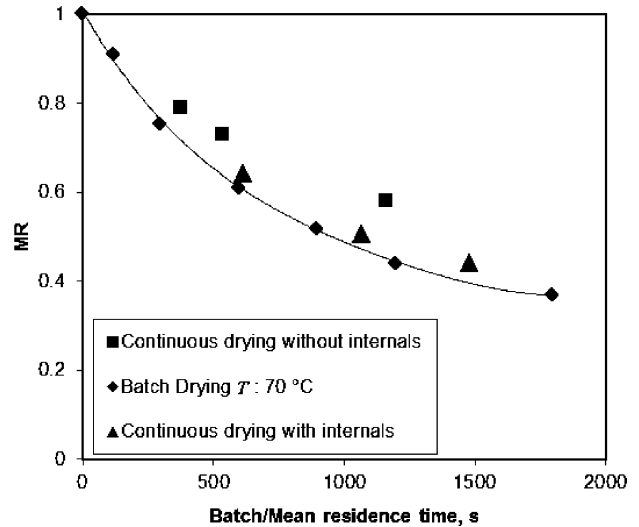
hensively compares the drying kinetics of the continuous dryers with the batch fluidized bed drier. The drying rate of solids in the continuous bed was found to be lower than the drying rate in a batch fluidized bed. These observations have been well recorded in literature[3], and attributed to the axial dispersion of solids in the bed due to the complete mixed nature of the fluidized beds. The drying rate of solids in the continuous spiral fluidized beds is approximately found to match with the batch drying rate as expected, since the axial mixing of the solids is very much reduced in a spiral bed. The reduction in axial mixing of solids in the spiral bed has been reported[31] for spiral fluidized beds.

The performance of continuous fluidized bed dryer with and without internals was predicted from the batch drying kinetics and the solids residence time distribution, as detailed in eq. (5). The use of batch kinetics and residence time distribution to predict the drying kinetics in the continuous fluidized beds has been duly reported in literature,[1]

$$\frac{C}{C_i} = \int_0^\infty \left(\frac{C}{C_i}\right)_{batch} E(\theta)\,d(\theta) \qquad (5)$$

The drying rate in a single stage continuous fluid bed drier can be predicted using residence time distribution function with the assumption of ideal mixing of solids in the fluidized bed, i.e.

$$E(\theta) = \exp(-\theta) \qquad (6)$$

The drying rate in a single-stage continuous spiral fluidized drier was predicted based on the correlation developed by Pydisetty *et al.*[30] for the

axial dispersion coefficient and residence time distribution function as given below,

$$E(\theta) = \sqrt{\frac{Pe}{4\pi}} \frac{1}{\theta^{3/2}} \exp\left[\frac{(1-\theta)^2 Pe}{4\theta}\right] d\theta \quad (7)$$

where the axial dispersion number was related to the system variables as,

$$\frac{D_e}{u_s d_p} = 450 \left[\frac{u_s}{u_g}\right]^{0.3} Fr^{0.7} Ar^{-0.7} \left[\frac{h}{d_p}\right]^{0.1} \quad (8)$$

The relative moisture content of solids leaving the single-stage spiral fluidized bed was predicted using eqs. (5), (7) and (8). The close correspondence of the experimental data with the model prediction warrants the use of batch kinetics and the residence time distribution for the prediction of drying kinetics in continuous fluidized beds.

Conclusion

Spirals as internals were utilized to reduce the axial mixing of solids in fluidized beds. The internals shift the solids flow from a completely mixed pattern to a plug flow type by reducing the back-mixing of solids. The drying rate in the continuous drying was estimated using the mean residence time of solids and found to increase with increase in the temperature of the heating medium and height of the downcomer (solids holdup). The drying rate in a continuous fluidized bed was lower than batch fluidized bed, while the drying rate in continuous fluidized bed with internals approximated the drying rate in batch fluidized bed. The kinetic performance of continuous drying of solids with and without internals was modeled using the batch drying kinetics and residence time distribution of solids in the fluidized beds. The batch drying kinetics was fitted with different semi-empirical models to estimate the kinetic parameters. Among the models tested, the Page model was found to match the experimental data, with minimum error. The kinetic parameter (k) was found to increase with temperature and the activation energy (E) was estimated to be 30.5 kJ mol^{-1}, while the Arrhenius constant (k_0) was 0.03 s^{-1}.

Nomenclature

C – average moisture content of ragi, kg kg^{-1}

C_i – initial moisture content of ragi, kg kg^{-1}

C_e – equilibrium moisture content, kg kg^{-1}

d_p – diameter of ragi particles, m

D_e – axial dispersion coefficient, m^2 s^{-1}

u_s – superficial solids velocity, m s^{-1}

u_g – superficial inlet air velocity, m s^{-1}

Fr – Froude number, $u_g^2 \, g^{-1} \, d_p^{-1}$

Ar – Archimedes number, $g d_p^3 \, \rho_g (\rho_s - \rho_g)/\mu^2$

ρ_s – density of ragi, kg m^{-3}

ρ_g – density of inlet air, kg m^{-3}

μ – viscosity of air, kg m^{-1} s^{-1}

$E(\theta)$ – exit age distribution function for solids

g – gravitational constant, m s^{-2}

G_s – solids flow rate, kg s^{-1}

L – length of the spiral, m

Pe – Peclet number, $u_s L/D_e$

h – height of the downcomer, m

θ – dimensionless time, $t/\bar{t}$

$\bar{t}$ – mean residence time of solids, ε_s / G_s

V_f – air flow rate, m^3 s^{-1}

ε_s – solids holdup, kg

References

1. *Strumillo, C., Kudra, T.,* Drying: Principles, Applications and Design. Gordon and Breach, New York, 1987.
2. *Srinivasakannan, C., Subbarao, S., Varma, Y. B. G.,* Powder Technology **78** (3) (1994) 203.
3. *Chandran, A. N., Subbarao, S., Varma, Y. B. G.,* AIChE J. **36** (1) (1990) 29.
4. *Srinivasakannan, C., Balasubramanian, N.,* Chemical Engineering and Technology **21** (1998) 961.
5. *Srinivasakannan, C.,* Int. J. of Food Engineering **4** (3) (2008) 1.
6. *Mckenzie, K. A., Bahu, R. E.,* Material model for fluidised bed drying. In Drying 91; *Mujumdar, A. S., Filkova, I.*, (Eds.); Elsevier, NewYork, 130, 1991.
7. *Srinivasakannan, C., Thomas, P. P., Varma Y. B. G.,* Industrial and Engineering Chemistry Research **34** (1995) 3068.
8. *Henderson, S. M.,* Transactions of the ASAE **17** (1974) 1167.
9. *Yaldiz, O., Ertekin, C., Uzun, H. I.,* Energy **26** (2001) 457.
10. *Duke, J. A.,* The quest for tolerant germplasm. In: ASA Special Symposium 32, Crop tolerance to suboptimal land conditions. Am. Soc. Agron. Madison, W.I., 1978, 1–61.
11. *Bogdan, A. V.,* Tropical pasture and fodder plants, Longman, London, 1977.
12. *Sharaf-Eldeen, Y. I., Blaisdell, J. L., Hamdy, M. Y.,* Transaction of the ASME **23** (1980) 1261.
13. *Kudras, T., Efremov, G. I.,* Drying Technology **21** (6) (2003) 1077.
14. *Topuz, M., Gur, M. Z., Gul.,* Applied Thermal Engineering **24** (2004) 1534.
15. *Hajidavalloo, E., Hamdullahpur., F.,* Mathematical modeling of simultaneous heat and mass transfer in fluidized bed drying of large particles, in Proceedings of CSME Form; Symposium on Thermal and Fluids Engineering, Toronto, Canada, 1988, 19–21.
16. *Ukan, G., Ulku, S.,* Drying of corn grains in batch fluidized bed. In Drying of Solids; *Mujumdar, A. S.,* (Ed.); Wiley Eastern Limited: New Delhi, 1986, 91–96.
17. *Mujumdar, A. S.,* Handbook of Industrial drying; Marcel Dekker: New York, 1987.
18. *Diamante, L. M., Munro, P. A.,* Solar Energy **51** (1993) 271.

19. *Zhang, Q., Litchfield, J. B.,* Drying Technology **9** (1991) 383.

20. *Henderson, S. M.,* Transactions of the ASAE **17** (1974) 1167.

21. *Yaldiz, O., Ertekin, C., Uzun, H. I.,* Energy **26** (2001) 457.

22. *Sharaf-Eldeen, Y. I., Blaisdell, J. L., Hamdy, M. Y.,* Transactions of the ASME **23** (1980) 1261.

23. *Srinivasakannan, C., Balasubramanian, N.,* Advanced Powder Technology **20** (4) (2009) 390.

24. *Vega, V., Fito, P., Andres, A., Lemus, R.,* Journal of Food Engineering **79** (2007) 146.

25. *Faustino, J. M. F., Barroca, M. J., Guine, R. P. F.,* Trans IChemE, Part C, Food and Bioproducts Processing **85** (C3) (2007) 163.

26. *Doymaz, I.,* Journal of Food Engineering **69** (2005) 161.

27. *Doymaz, I., Pala, M.,* Journal of Food Engineering **60** (2003) 125.

28. *Kitic, D., Viollaz, P. E.,* Journal of Food Technology **19** (1984) 399.

29. *Doymaz, I.,* Journal of Food Engineering **61** (2004) 359.

30. *Pydisetty, Y., Krishnaiah, K., Varma, Y. B. G.,* Powder Technology **59** (1989) 100.